BPB Reports

Regular Article

Increased Expression of Heparan Sulfate 6-O-Sulfotransferase-2 Promotes Collagen Production in Cardiac Myofibroblasts

Kotaro Kasai,[a,b] Yuma Horii,[a,b] Takanori Hironaka,[a,b] Kyosuke Mae,[b] Tomoyuki Ueno,[b] Akiomi Nagasaka,[b] and Michio Nakaya*[a,b]

[a]*Department of Disease Control;* [b]*Department of Pharmacology and Toxicology, Graduate School of Pharmaceutical Sciences, Kyushu University, Maidashi 3-1-1, Higashiku, Fukuoka, Fukuoka 812-8582, Japan*
Received April 22, 2021; Accepted May 14, 2021

Fibrosis is defined as the excessive accumulation of extracellular matrix (ECM) proteins. These excessive ECM proteins are produced by myofibroblasts, which are differentiated mainly from resident fibroblasts in response to tissue injury. In addition to the ECM proteins, the amounts of heparan sulfate, one of the sugar chains, and the proteoglycans attached with heparan sulfate chains are reported to be increased in the fibrotic tissues. However, the contribution of heparan sulfate and heparan sulfate proteoglycans to the development of fibrosis remains unclear. In this study, we found that heparan sulfate 6-O-sulfotransferase-2 (Hs6st2), a type of heparan sulfate transferase, is remarkably induced during fibrosis in the heart, liver, and kidney of mice. We also demonstrated that *Hs6st2* was specifically expressed in myofibroblasts of mice with cardiac and liver fibrosis. *Hs6st2* knockdown in cardiac myofibroblasts reduced the mRNA expression of fibrosis-related factors, such as Collagen1a1. In summary, this study revealed that *Hs6st2* is specifically expressed in myofibroblasts in fibrotic tissues, promotes fibrosis, and can be a good target for the treatment for fibrosis.

Key words myofibroblast, fibrosis, heparan sulfate 6-O-sulfotransferase-2

INTRODUCTION

Fibrosis is a pathological process common to a variety of tissues and diseases. It is defined as the excessive accumulation of the extracellular matrix (ECM), such as collagen and fibronectin, in the inflamed or damaged tissue, which can give rise to organ dysfunction.[1,2] Although fibrosis is becoming increasingly recognized as a main cause of mortality in many diseases, there are few treatment strategies that can arrest or reverse fibrosis.[1,2]

Myofibroblasts are the primary cells that produce and secrete greater levels of ECM proteins during fibrosis.[3] In inflamed or damaged tissue, resident fibroblasts in the tissue mainly differentiate into myofibroblasts due to the stimulation of cytokines represented by transforming growth factor beta (TGF-β), secreted by macrophages.[4,5] Although, to date, much effort has been paid to elucidate the molecular mechanisms that regulates the overproduction of ECM proteins, the understanding of the mechanisms is still limited.

Heparan sulfate proteoglycans are glycoconjugates in which sulfated sugar chains called heparan sulfate are attached to the core proteins.[6,7] The heparan sulfate chain has a linear backbone composed of repeating disaccharides of glucuronic acid and N-acetylglucosamine.[6,7] Heparan sulfate proteoglycans are involved in a variety of signaling pathways, such as growth factors and morphogenetic factors, which act as modulators that regulate the association of ligand molecules and receptors, and the storage and release of ligand molecules.[7,8] In the fibrotic tissues, the amount of heparan sulfate[9] and the expression levels of some heparan sulfate proteoglycans, such as Syndecan-1,[10–12] Glypican-3,[13] and Perlecan,[14] were reported to be increased. Syndecan-1 was also demonstrated to promote fibrosis in various tissues.[10–12] These reports suggested the physiological significance of heparan sulfate modification in fibrosis.

Heparan-sulfate 6-O-sulfotransferase (HS6ST) family, one of the heparan sulfate synthases, is an enzyme that catalyzes the sulfation of N-sulfoglucosamine at position 6.[15,16] HS6ST family proteins are composed of three subtypes, HS6ST1, HS6ST2, and HS6ST3.[17] A recent study has shown that the elevated expression of HS6ST1 is closely associated with the condition in the lungs of patients with idiopathic pulmonary fibrosis.[18] However, the involvement of HS6ST2 and HS6ST3 in fibrosis has not been clarified. In this study, we explored the biological function of HS6ST2 in fibrosis.

MATERIALS AND METHODS

Mice C57BL/6J mice were purchased from Japan SLC Inc. (Shizuoka, Japan). All mice studies were approved by the Animal Care and Use Committee of Kyushu University and followed the relevant national and international guidelines in the 'Act on Welfare and Management of Animals' (Ministry of Environment of Japan).

Myocardial Infarction (MI) Model Male mice (8–10 weeks old) were anesthetized and subjected to permanent occlusion of the left coronary artery. For comparison, mice were subjected to the same procedure without the occlusion and these mice

*To whom correspondence should be addressed. e-mail: nakaya@phar.kyushu-u.ac.jp

was defined as 'sham' group.

Non-Alcoholic Steatohepatitis (NASH) Model Male mice (6 weeks old) were fed a choline-deficient, L-amino acid-defined high-fat diet with 60 kcal% fat and 0.1% methionine (CDAHFD) (Research Diets, NB, USA) for 10 weeks. For comparison, mice that were fed a normal diet (Research Diets) for 10 weeks were analyzed.

CCl_4-Induced Liver Fibrosis Model Male mice (8–10 weeks old) were intraperitoneally administered CCl_4 [1 μL/g (Sigma-Aldrich, MO, USA), dissolved in corn oil (Sigma-Aldrich)], twice weekly for 4 weeks. For comparison, mice were administered vehicle (corn oil) and these mice was defined as 'sham' group. In addition, we prepared mouse group bred for more 4 weeks after the final CCl_4 administration (termed as 'Recover' group).

Unilateral Ureteral Obstruction (UUO) Model Anesthetized female mice (8–10 weeks old) were subjected to permanent occlusion of the left ureter. For comparison, mice that received the same procedure without the occlusion were analyzed. Ten days after the UUO operation, the kidneys of the mice were collected.

Real-Time RT-PCR Analysis Total RNA from the tissues was collected by Isogen (Nippon gene, Tokyo, Japan) and purified using RNeasy Plus Mini Kit (QIAGEN, NRW, Germany). Total RNA from myofibroblasts was isolated using RNeasy Plus Mini Kit (QIAGEN). cDNA was synthesized using High-capacity cDNA Reverse Transcription Kit (Thermo Fisher Scientific, MA, USA). Real-time RT-PCR was performed using Luna Universal qPCR Master Mix (New England BioLabs, MA, USA) on a StepOnePlus Real-Time PCR system (Applied Biosystems, CA, USA). Real-time RT-PCR probes were purchased from Applied Biosystems or Sigma-Aldrich and are described below.

Mouse *Gapdh* (Forward: 5′-CGTCCCGTAGACAAAATGGTGA-3′, Reverse: 5′-CCACTTTGCCACTGCAAATGG-3′, Probe: 5′-FAM-CCAATACGGCCAAATCCGTTCACACCGA-TAMRA-3′),

Mouse *Hs6st1* (Forward: 5′-TGCGTTCGCCCAGAAAGTTC-3′, Reverse: 5′-GTCGCCATTCACTCAGGTAGC-3′, Probe: 5′-FAM-ATCACCCTGCTGCGAGACCCCGTATTAMRA-3′),

Mouse *Hs6st2* (Forward: 5′-GCCAACAACCGCCAAGTTC-3′, Reverse: 5′-AACGCCATGTGCTTCAGATTG-3′, Probe: 5′-FAM-TGACCTGACTCTAGTGGGATGCTACAACCT-TAMRA-3′),

Mouse *Hs6st3* (Forward: 5′-CCACAGCCACACCAGGAATTT-3′, Reverse: 5′-GGACATGCTTCCATTCGCTCA-3′, Probe: 5′-FAM-TGACACTGGGTCCCGCAACATCGTGA-3′),

Mouse *Cd68* (Forward: 5′-CCGCTTATAGCCCAAGGAACA-3′, Reverse: 5′-TTCTGTGGCTGTAGGTGTCATC-3′, Probe: 5′-FAM-AAAGGCCGTTACTCTCCTGCCATCCT-TAMRA-3′),

Mouse *Acta2* (Forward: 5′-CACCATGAAGATCAAGATCATTGCC-3′, Reverse: 5′-GGTAGACAGCGAAGCCAGGA-3′, Probe: 5′-FAM-AGCCACCGATCCAGACAGAGTACTTGCG-TAMRA-3′),

Mouse *Col1a1* (Forward: 5′-CCCAAAGGTTCTCCTGGTGAAG-3′, Reverse: 5′-CGGTTTTGCCATCAGGACCA-3′, Probe: 5′-FAM-TGGTGCCAAGGGTCTCACTGGCAGTCTAMRA-3′),

Mouse *Col8a1* (Forward: 5′-CGAGAGGGGAAAAAGGACCCA-3′, Reverse: 5′-TGGTCCTACAACTCCACCTTCTC-3′, Probe: 5′-FAM-AGGTGCTATTGGTTTCCCTGGACCCA-TAMRA-3′),

Mouse *Lox* (Forward: 5′-CAAGCTGGTTTCTCGCCGTC-3′, Reverse: 5′-TGTAGGGGTCGTCGCCCA-3′, Probe: 5′-FAM-ATCGCCACAGCCTCCGCAGCTCAGTAMRA-3′),

Mouse *Il6* (Forward: 5′- TGGAAATGAGAAAAGAGTTGTGC-3′, Reverse: 5′- TCCAGTTTGGTAGCATCCATCA-3′, Probe: 5′-FAM- TTCTGCAAGTGCATCATCGTTGTTCATACA-3′),

Mouse *Cyp7a1 Mm00484150_m1*

Relative gene expression was determined using the comparative Ct method. *Gapdh* mRNA was amplified as an internal control. In the absolute quantification of *Hs6st1* or *Hs6st2* mRNA, pMD20-*Hs6st1* (NM_015818.2, coding sequence of 282–853 bp) and pMD20-*Hs6st2* (NM_001290467.1, coding sequence of 934–1500 bp) were used to create standard curves. The copy numbers of *Hs6st1* and *Hs6st2* in 1 ng RNA were determined from the standard curves.

Isolation of Cardiac Myofibroblasts by Magnetic-Activated Cell Sorting (MACS) The hearts of the mice were collected three days after the MI operation and digested using 0.1% Collagenase type II (Worthington, NJ, USA), 0.01% Elastase (Worthington), and 2.5 mg/mL DNase I (Sigma Aldrich) in phosphate-buffered saline (PBS) (Nacalai Tesque, Kyoto, Japan) at 37°C for 1 h under shaking. The cells were collected and treated with red blood lysis buffer (Roche, BL, Swiss) and plated in Dulbecco's modified eagle's medium (Nacalai Tesque), containing 10% fetal bovine serum (Thermo Fisher Scientific) and 1% penicillin-streptomycin (Nacalai Tesque) for 6 h. Then, the culture medium was exchanged with fresh medium, and the cells were allowed to grow overnight at 37°C. After overnight culture, the cells were collected by accutase (Nacalai Tesque) treatment, washed using MACS buffer (0.5% bovine serum albumin [BSA]/2 mM EDTA (DOJINDO, Kumamoto, Japan)/PBS), and incubated with CD45 microbeads on ice for 20 min (Miltenyi Biotec, NRW, Germany). The CD45-negative cells were isolated using MACS column and were used as cardiac myofibroblasts.

Isolation of Hepatocytes, Kupffer Cells, and Hepatic Stellate Cells (HSCs) by MACS After the 4-week-administration of CCl_4, the livers of mice were perfused with wash buffer [25 mM HEPES (DOJINDO)/0.5 mM EDTA/HBSS (Nacalai Tesque)] at 37°C through the portal vein and subsequently with digestion buffer [0.1% Collagenase A (Roche)/1.5 mM HEPES/HBSS]. Next, the livers were collected and digested in digestion buffer at 37°C for 30 min. The cells were subjected to centrifugation [50 × g, 1 min] twice, and divided into the precipitated cell fraction and the supernatant cell fraction. The precipitated cell fraction was collected and plated on a 0.1% (w/v) gelatin-coated dish for 6 h. The adherent cells were collected by accutase treatment, and washed using MACS buffer, followed by incubation with CD45 microbeads on ice for 20 min. The CD45-negative cells were isolated using MACS column and were then used as hepatocytes. The supernatant cell fraction was separated using F4/80 microbeads (Miltenyi Biotec) and the F4/80-positive cells were collected as Kupffer cells. The F4/80-negative cells were incubated with CD45 microbeads and subsequently subjected to MACS separation. CD45-negative cells were collected as HSCs.

***In situ* Hybridization** Seven days after the MI operation,

the hearts of the mice were fixed in 4% paraformaldehyde (Nacalai Tesque) overnight, frozen with Tissue-Tek O.C.T. Compound (Sakura, Tokyo, Japan), and cut into 6-μm sections. The sections were subjected to RNAScope® Multiplex Fluorescent v2 Assay kit (Advanced Cell Diagnostics, CA, USA) using RNAScope® probe specific for *Hs6st2,* according to the manufacturer's instructions. Subsequently, the sections were incubated with blocking buffer (10% BSA/PBS) and incubated with rabbit anti-αSMA antibody (1:200; ab5694, abcam, Cambs, England) or rat anti-CD45 antibody (1:200; 103119, Biolegend, CA, USA), diluted in blocking buffer, overnight at 4°C. After PBS wash, the sections were incubated with Alexa488-conjugated donkey anti-rabbit IgG antibody (1:200; A-21206, Invitrogen, CA, USA) or Alexa488-conjugated donkey anti-rat IgG antibody (1:200; A-21208, Invitrogen), diluted in blocking buffer, for 1 h at 20°C, washed using PBS, and incubated with 4′,6-diamidino-2-phenylindole (1:1000, DOJINDO), diluted in PBS, for 5 min. After PBS wash, the sections were sealed and observed using confocal microscope (LSM700).

Knockdown Analysis Myofibroblasts were treated with small interfering RNA (siRNA) (50 pmol, mouse *Hs6st2*: s78481 control: 4390844, life technologies, CA, USA) using Lipofectamine™ RNAiMAX (Invitrogen). Total RNA was isolated 48 h later.

Statistical Analysis The statistical analyses were performed using PRISM 5 (GraphPad Prism software, CA, USA). The results were described as the means ± standard error of mean. The results were statistically analyzed using the unpaired Student's t-test or one-way ANOVA, followed by Tukey's multiple comparison tests.

RESULTS

***Hs6st2* Expression was Remarkably Increased in Fibrotic Heart, Liver, and Kidney** To examine the contribution of *Hs6st* family members to cardiac fibrosis, we first examined the mRNA expression levels of *Hs6st* family members, *Hs6st1*, *Hs6st2*, and *Hs6st3* in the hearts of mice after MI treatment, which is known to induce cardiac cell death, resulting in the inflammation and fibrosis in the heart. We found that the mRNA level of *Hs6st1* was expressed in the healthy mouse hearts (Fig. 1A), and the expression level of *Hs6st1* was significantly increased in the infarct region but not in non-infarct region of the hearts of mice, 3 or 7 d after MI (Fig. 1B). In contrast, *Hs6st2* was hardly expressed in healthy mouse hearts (Fig. 1A). However, its expression was greatly increased in the infarct region, but not in non-infarct region of the hearts of mice 3, 7, or 28 d after MI (Fig. 1B). The increased expression of *Col8a1* in the infarct region of the hearts of mice 3, 7, or 28 d after MI confirmed that fibrotic responses occurred in the region (Fig. 1B). *Hs6st3* was not expressed in healthy or infarcted hearts of mice (data not shown). These results suggested that the increase in the mRNA expression of *Hs6st1* and *Hs6st2* was linked to cardiac fibrosis.

We then examined whether the increase in the mRNA expression levels of *Hs6st1* and *Hs6st2* was also observed in hepatic fibrosis. Male mice were fed a CDAHFD for 10 weeks to induce a mouse model of NASH with fibrosis. Results from the real-time RT-PCR analysis revealed that *Hs6st1* was expressed in normal mouse liver fed with standard diet (Fig. 1C), and its expression level was not increased in NASH mouse liver (Fig. 1D). In contrast, *Hs6st2* was not expressed in normal mouse liver (Fig. 1C), and the expression levels of *Hs6st2* and *Col8a1* were strikingly increased in NASH mouse liver (Fig. 1D). *Hs6st3* was not expressed in healthy or NASH livers of mice (data not shown).

In addition, the mRNA expression of *Hs6st2* and *Col8a1* were greatly increased in the fibrotic liver of mice after 4 weeks of administration of CCl_4, which is known to induce liver injury (Fig. 1E). The liver is a highly regenerative organ. It was observed that the livers of mice that were bred for 4 more weeks after the final CCl_4 administration were quite similar to the normal mouse liver. Interestingly, 4 weeks after withdrawal of CCl_4 administration, *Hs6st2* and *Col8a1* mRNA expressions were significantly reduced, reaching to the level in the vehicle group (Fig. 1E). These findings suggested that the expression level of *Hs6st2* was correlated with the extent of hepatic fibrosis.

We further examined the increase in the expression of *Hs6st1* and *Hs6st2* in fibrotic kidney. For the experiment, we used an UUO model, which is a widely used model of renal fibrosis. As observed in case of the liver, the expression level of *Hs6st1* was not altered in fibrotic kidney, while that of *Hs6st2* and *Col8a1* were greatly increased (Fig. 1F). *Hs6st3* was not expressed in healthy or UUO kidneys of mice (data not shown). Taken together, these results indicated that *Hs6st2* mRNA expression was increased in the fibrotic heart, liver, and kidney of mice.

***Hs6st2* was Specifically Expressed in the Myofibroblasts of Fibrotic Heart of Mouse** We then examined the cells that express *Hs6st2* in the fibrotic heart of mice by *in situ* hybridization. In the section of mice hearts after sham operation, the signals for *Hs6st2* mRNA were rarely detected (Fig. 2A). In contrast, the signals were abundant in infarct area of the mice hearts, 7 d after MI. Close observation of the sections also revealed that the signals for *Hs6st2* mRNA were exclusively found in the interstitium of the infarcted mice hearts. The main population of the cells that reside in the interstitium of the infarcted mice hearts are myofibroblasts or leukocytes, though the number of myofibroblasts is much larger than that of leukocytes. Therefore, we examined whether these cells express *Hs6st2*. *In situ* hybridization to detect *Hs6st2* mRNA, and the immunostaining for alpha smooth muscle actin (αSMA), a marker of myofibroblasts, were performed on the same heart sections. We found that almost all *Hs6st2* signals were detected in the myofibroblasts (Fig. 2B). However, the signals were not found in the cells that express CD45, a marker of leukocytes (Fig. 2C). αSMA is the most commonly used marker molecule for myofibroblasts, but it is well known that αSMA is more highly expressed in smooth muscle than in myofibroblasts. Interestingly, we found that *Hs6st2* was not expressed in the vascular smooth muscle cells present around the vessel, suggesting that *Hs6st2* may be a better marker molecule than αSMA, at least in the fibrotic hearts of mice (Fig. 2D).

We further examined whether *Hs6st2* was also expressed in myofibroblasts of fibrotic livers. Since it was technically difficult to perform *in situ* hybridization using the livers of NASH mice and CCl_4-treated mice, we fractionated the cell population of hepatocytes, Kupffer cells (liver macrophages), and hepatic stellate cells (liver myofibroblasts) by centrifugation and MACS. We confirmed the purity of hepatocytes, Kupffer cells, and myofibroblasts by measuring the mRNA expression levels of *Cyp7a1* (a hepatocyte marker), *Cd68* (a macrophage

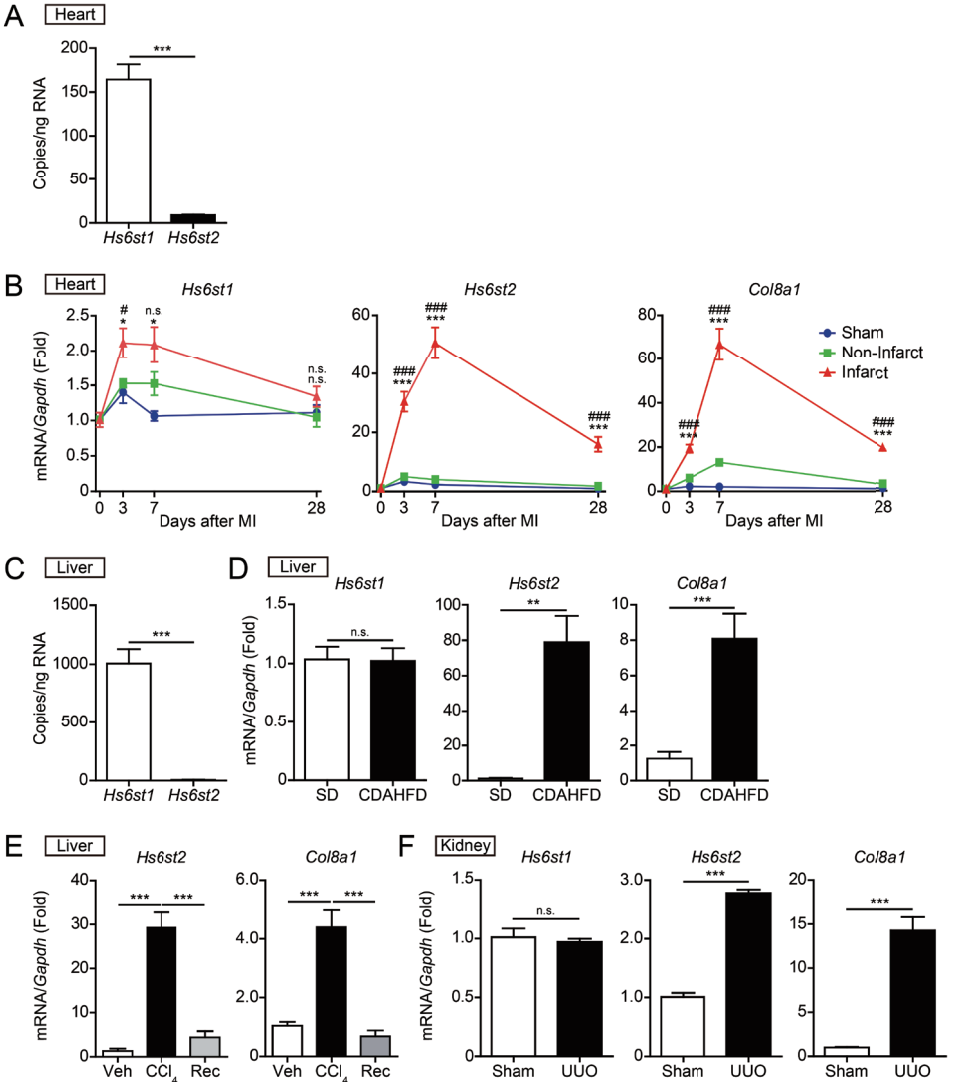

Fig. 1. The mRNA Expression Levels of *Hs6st2* were Significantly Increased in the Fibrotic Heart, Liver, and Kidney of Mice

(A) Absolute quantification of the gene expression of *Hs6st1* and *Hs6st2* in healthy mouse hearts by real-time RT-PCR (n = 3 each). (B) The mRNA expression levels of *Hs6st1*, *Hs6st2*, and *Col8al* in mouse hearts 0, 3, 7, and 28 d after MI operation. 'Sham' means sham-operated mouse hearts. 'Infarct' or 'Non-infarct' means infarct region or non-infarct region of mouse hearts after MI. ***$P < 0.001$, *$P < 0.05$ Infarct vs Sham. ###$P < 0.001$, #$P < 0.05$ Infarct vs Non-infarct. n = 3–6. (C) Absolute quantification of the gene expression of *Hs6st1* and *Hs6st2* in livers of mice fed with a standard diet by real-time RT-PCR (n = 7 each). (D) The mRNA expression levels of *Hs6st1*, *Hs6st2*, and *Col8al* in the livers of mice fed with a standard diet (SD) or mice with CDAHFD-induced NASH (n = 4–7). (E) The mRNA expression levels of *Hs6st2* and *Col8al* in livers of mice after 4 weeks of administration of corn oil, used as vehicle (Veh) or CCl_4, or livers CCl_4-administered mice after 4 weeks recovery (Rec) (n = 5–6). (F) The mRNA expression levels of *Hs6st1*, *Hs6st2*, and *Col8al* in the kidneys of mice after sham or UUO operation (n = 5). The mRNA levels were normalized to those of *Gapdh* (B, D–F) and shown as fold changes relative to day 0 (B), SD (D), Veh (E) or Sham (F). Data are presented as the mean ± SEM. For (A–F), ***$P < 0.001$, **$P < 0.01$, n.s.: not significant.

marker), and *Acta2* (encodes αSMA) (Fig. 2E). Results from the real-time RT-PCR analysis revealed that *Hs6st2* expression was only detected in the myofibroblast population, indicating that *Hs6st2* was also expressed in myofibroblasts of fibrotic livers (Fig. 2E).

***Hs6st2* Knockdown Attenuated the Expression of Fibrosis-Related Genes in Cardiac Myofibroblasts** We finally investigated the role of *Hs6st2* in cardiac myofibroblasts. Comparison of *Hs6st1* and *Hs6st2* mRNA expression levels in the cardiac myofibroblasts, using absolute quantification methods, revealed that the mRNA expression level of *Hs6st1* was markedly lower than that of *Hs6st2* (Fig. 3A). Since the main function of cardiac myofibroblasts is the production of extracellular matrix proteins, we examined the effect of *Hs6st2* on their production. For this purpose, we treated cardiac myofibroblasts with siRNA targeting *Hs6st2* and measured the mRNA expression levels of *Col1a1*, *Col8a1*, and *Lox* by real-time RT-PCR analysis. The analysis demonstrated that their expression levels were significantly decreased by *Hs6st2* knockdown (Fig. 3B). On the other hand, the expression level of *Il6*, an inflammatory gene, was not changed by *Hs6st2* knockdown (Fig. 3C). These results implied that *Hs6st2* enhances the fibrosis by increasing the expression of collagen genes in cardiac myofibroblasts.

DISCUSSION

We demonstrated that *Hs6st2* expression was markedly increased during fibrosis in the heart, liver, and kidney of mice. *Hs6st2* was hardly expressed in the normal mouse heart but was specifically expressed in myofibroblasts of the fibrotic hearts after MI. *Hs6st2* expressed in the myofibroblasts was

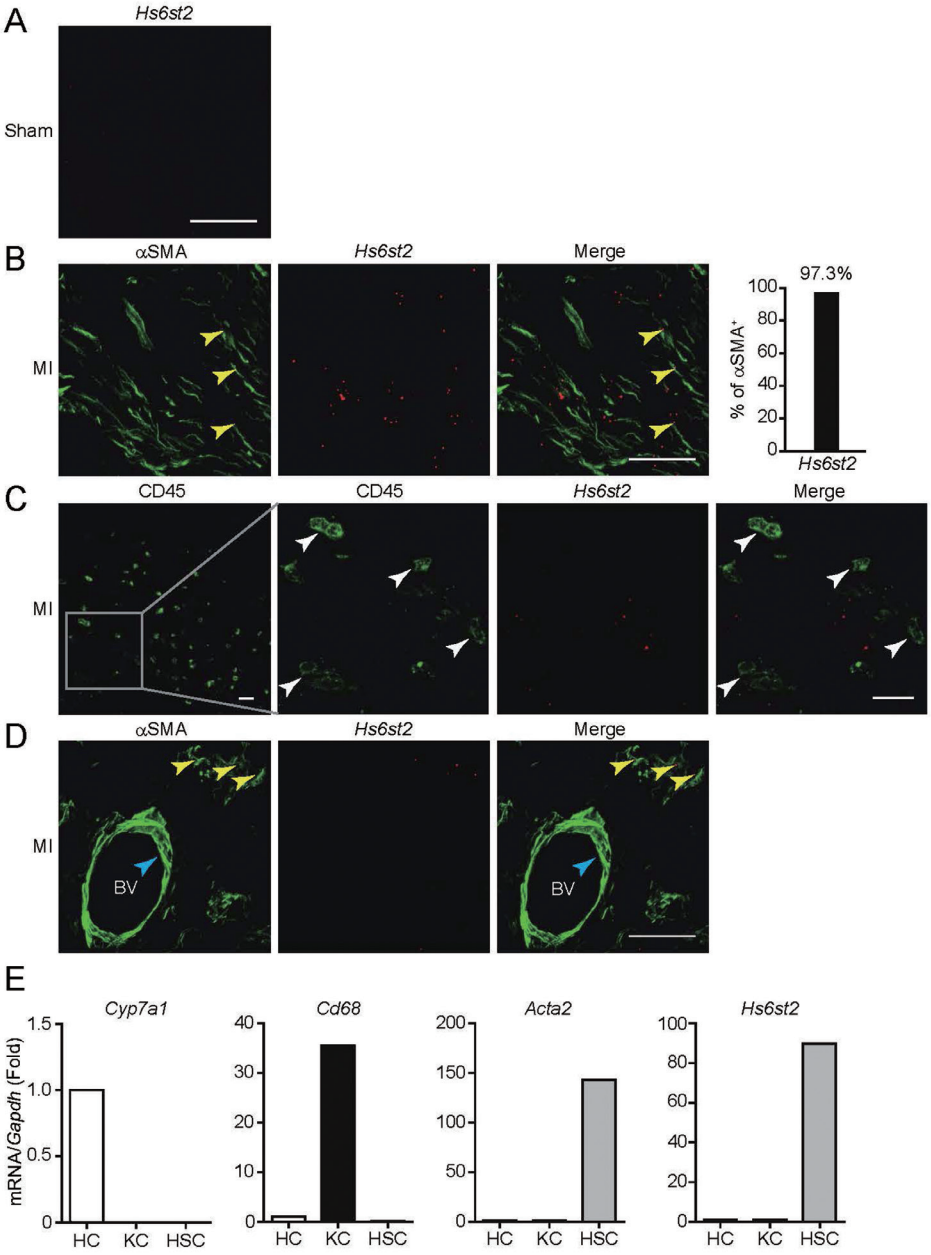

Fig. 2. *Hs6st2* is Specifically Expressed in Cardiac Myofibroblast and Hepatic Stellate Cells

(A–D) Representative *in situ* hybridization images detecting *Hs6st2* mRNA in mice left ventricle of sham (A) or 7 d after MI operation (B–D). The sections were co-stained with an anti-αSMA (green) (B, D) or anti-CD45 (green) (C) antibody. Yellow arrowheads indicate the signals for *Hs6st2* (red) detected in myofibroblasts that express αSMA. The percentage of the *Hs6st2*-positive cells (n = 150) that are also αSMA-positive were quantified and shown in a graph. White arrowheads indicate leukocytes. Blue arrowheads indicate vascular smooth muscle cells. BV in the images of (D) indicates the blood vessels. Scale bars in (A–D) = 20 μm. (E) The mRNA expression levels of *Cyp7a1, Cd68, Acta2* and *Hs6st2* in hepatocytes (HC), Kupffer cells (KC) and hepatic stellate cells (HSC) isolated from a CCl_4-induced fibrotic mouse liver (n = 1). mRNA levels were normalized to those of *Gapdh* and shown as fold changes relative to HC.

found to promote the production of extracellular matrix proteins, such as collagen.

Cardiac myofibroblasts are reported to differentiate primarily from resident fibroblasts present in the normal heart.[5] Since *Hs6st2* is not expressed in the resident fibroblasts in the normal mouse heart, the mRNA expression of *Hs6st2* is considered to increase with the differentiation from the resident fibroblasts into myofibroblasts. One of the important signals for myofibroblast differentiation is TGF-β signaling.[4] Therefore, *Hs6st2* expression may be regulated by TGF-β signaling. In contrast to the expression of *Hs6st2*, the expression of *Hs6st1*, a molecule belonging to the same *Hs6st* family, showed little change in during fibrosis (Fig. 1). Therefore, in cardiac fibroblasts/myofibroblasts, the expression levels of *Hs6st1* and *Hs6st2* were considered to be controlled by different mechanisms. Interestingly, it has been reported that unlike in cardiac myofibroblasts, the expression level of *Hs6st1* increases in lung myofibroblasts during pulmonary fibrosis, whereas the expression level of *Hs6st2* does not change in the cells.[18] At present, it is not clear why the types of *Hs6st* that increase in expression with fibrosis in the heart and lung are different. However, since both *Hs6st1* and *Hs6st2* have the function of

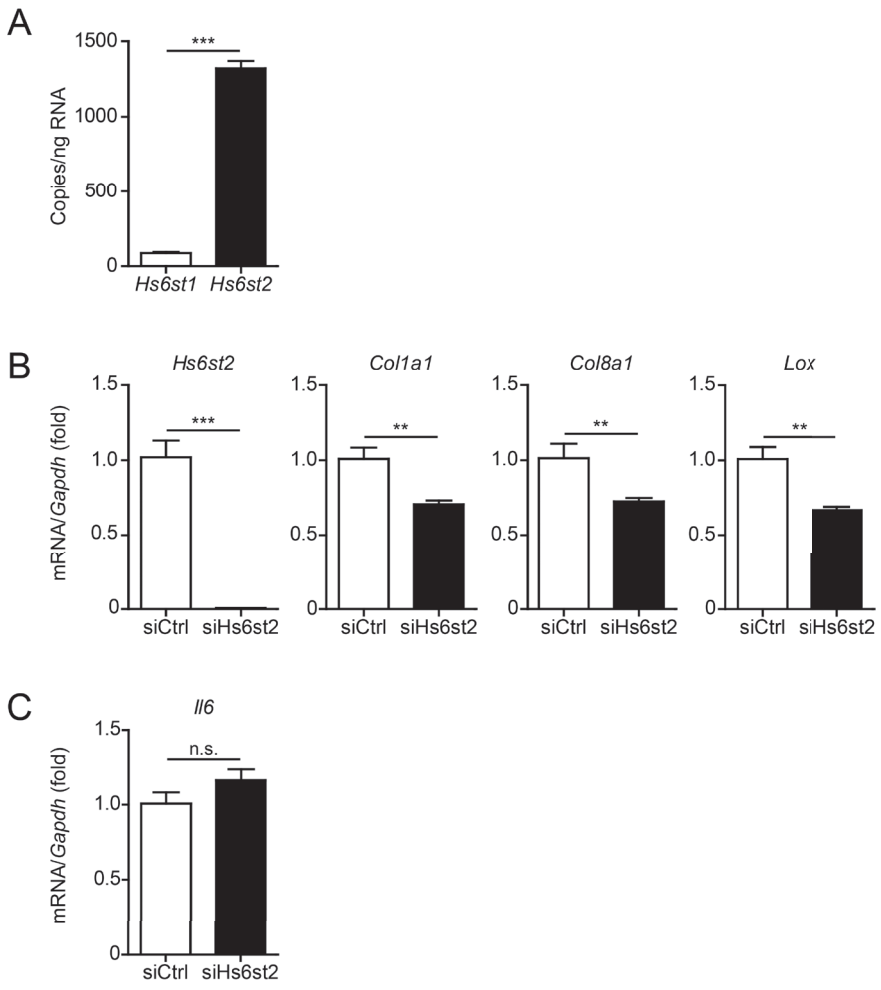

Fig. 3. *Hs6st2* Knockdown Decreases the Expression Levels of Fibrosis-Related Genes in Cardiac Myofibroblasts

(A) Absolute quantification of the gene expression of *Hs6st1* and *Hs6st2* in cardiac myofibroblasts by real-time RT-PCR (n = 5 each). (B) The mRNA expression levels of *Hs6st2*, *Col1a1, Col8a1,* and *Lox* in cardiac myofibroblasts after treatment of siRNA targeting *Hs6st2* or siCtrl (n = 5 each). (C) The mRNA expression level of *Il6* in cardiac myofibroblasts after treatment of siRNA targeting *Hs6st2* or siCtrl (n = 5 each). The mRNA levels were normalized to those of *Gapdh* and shown as fold changes relative to siCtrl. Data are presented as the mean ± SEM. ***$P < 0.001$, **$P < 0.01$, n.s.: not significant.

adding sulfate group to N-sulfoglucosamine,[15–17] it is considered that they may add sulfate group to N-sulfoglucosamine of the same proteins that promote collagen production in the fibrotic heart and lung. One of the candidate proteins is Syndecan-1, a heparan sulfate proteoglycan that is modulated by the HS6ST family.[19] Syndecan-1 is known to increase its expression in tissues with fibrosis.[10–12] Therefore, it may be interesting to detect the changes in the glycosylation of Syndecan-1 during the differentiation into myofibroblasts.

It has been known that *Hs6st2* promotes the signal transduction mediated by growth factors, such as epidermal growth factor (EGF) and fibroblast growth factor (FGF).[20,21] In fact, in the adipocytes of *Hs6st2* KO mice, in which increased lipid accumulation in liver was observed, FGF19 and 21 downstream signaling was attenuated.[22] The myofibroblast differentiation was promoted by various cytokines, such as TGF-β, platelet-derived growth factor (PDGF) and FGF.[23,24] Therefore, HS6ST2 may contribute to the myofibroblast differentiation by modulating these cytokine-elicited pathways. In this context, it would be interesting to examine whether the FGF downstream signaling was decreased in *Hs6st2* knock downed myofibroblasts.

In the heart, *Hs6st2* is expressed specifically in myofibroblast and it promotes the expression of fibrotic factors, such as collagen. The molecular mechanisms that regulate fibrosis in each tissue are still obscure, and the development of the effective drug for fibrosis is desired. Since *Hs6st2* is rarely expressed in the normal heart, liver, and kidney, it may be a good therapeutic target for fibrotic diseases with low risk of side effects.

Acknowledgments We would like to thank Dr. H. Kurose for his kind support throughout this research. This study was supported by grants from Grants-in-Aid for Scientific Research (KAKENHI) [to M.N. (JP22590083, JP25670120, JP20H03383) and A.N. (JP19K07122)]; The Takeda Science Foundation, The Mochida Memorial Foundation for Medical and Pharmaceutical Research, 2018 Bristol-Myers Squibb KK Research Grants, The Salt Science Research Foundation, The Koyanagi Foundation, The Nakatomi Foundation, The Suzuken Memorial Foundation (to M.N.); from Japan Agency for Medical Research and Development (AMED) (JP20gm5810030 to M.N.); from Grant-in-Aid for JSPS Research Fellow (JP19J20083 to Y.H., JP21J11273 to T.H.) ; from Platform Project for Supporting Drug Discovery and Life Science Research (Basis for Supporting Innovative Drug

Discovery and Life Science Research (BINDS)) from AMED under Grant Number JP19am0101091. We appreciate for the technical supports from the Research Support Center, Graduate School of Medical Sciences, Kyushu University and from Medical Institute of Bioregulation, Kyushu University.

Conflict of interest The authors declare no conflict of interest.

REFERENCES

1) Pellicoro A, Ramachandran P, Iredale JP, Fallowfield JA. Liver fibrosis and repair: immune regulation of wound healing in a solid organ. *Nat. Rev. Immunol.*, **14**, 181–194 (2014).
2) Henderson NC, Rieder F, Wynn TA. Fibrosis: from mechanisms to medicines. *Nature*, **587**, 555–566 (2020).
3) Hinz B, Phan SH, Thannickal VJ, Galli A, Bochaton-Piallat ML, Gabbiani G. The myofibroblast: one function, multiple origins. *Am. J. Pathol.*, **170**, 1807–1816 (2007).
4) Carthy JM. TGFβ signaling and the control of myofibroblast differentiation: implications for chronic inflammatory disorders. *J. Cell. Physiol.*, **233**, 98–106 (2018).
5) Kanisicak O, Khalil H, Ivey MJ, Karch J, Maliken BD, Correll RN, Brody MJ, Lin SCJ, Aronow BJ, Tallquist MD, Molkentin JD. Genetic lineage tracing defines myofibroblast origin and function in the injured heart. *Nat. Commun.*, **7** (2016).
6) Esko JD, Selleck SB. Order out of chaos: assembly of ligand binding sites in heparan sulfate. *Annu. Rev. Biochem.*, **71**, 435–471 (2002).
7) Nadanaka S, Kitagawa H. Heparan sulphate biosynthesis and disease. *J. Biochem.*, **144**, 7–14 (2008).
8) Sarrazin S, Lamanna WC, Esko JD. Heparan sulfate proteoglycans. *Cold Spring Harb. Perspect. Biol.*, **3** (2011).
9) Sasaki T, Kojima S, Kubodera A. Uptake of 67Ga in the lung of mice during bleomycin treatment. *Eur. J. Nucl. Med.*, **9**, 57–61 (1984).
10) Kliment CR, Englert JM, Gochuico BR, Yu G, Kaminski N, Rosas I, Oury TD. Oxidative stress alters syndecan-1 distribution lungs with pulmonary fibrosis. *J. Biol. Chem.*, **284**, 3537–3545 (2009).
11) Charchanti A, Kanavaros P, Koniaris E, Kataki A, Glantzounis G, Agnantis NJ, Goussia AC. Expression of syndecan-1 in chronic liver diseases: correlation with Hepatic fibrosis. *In Vivo*, **35**, 333–339 (2021).
12) Lunde IG, Herum KM, Carlson CC, Christensen G. Syndecans in heart fibrosis. *Cell Tissue Res.*, **365**, 539–552 (2016).
13) Udomsinprasert W, Angkathunyakul N, Klaikeaw N, Vejchapipat P, Poovorawan Y, Honsawek S. Hepatic glypican-3 and alpha-smooth muscle actin overexpressions reflect severity of liver fibrosis and predict outcome after successful portoenterostomy in biliary atresia. *Surgery*, **167**, 560–568 (2020).
14) Lord MS, Tang F, Rnjak-Kovacina J, Smith JGW, Melrose J, Whitelock JM. The multifaceted roles of perlecan in fibrosis. *Matrix Biol.*, **68–69**, 150–166 (2018).
15) Habuchi H, Habuchi O, Kimata K. Purification and characterization of heparan sulfate 6-sulfotransferase from the culture medium of Chinese hamster ovary cells. *J. Biol. Chem.*, **270**, 4172–4179 (1995).
16) Habuchi H, Kobayashi M, Kimata K. Molecular characterization and expression of heparan-sulfate 6- sulfotransferase. Complete cDNA cloning in human and partial cloning in Chinese hamster ovary cells. *J. Biol. Chem.*, **273**, 9208–9213 (1998).
17) Habuchi H, Tanaka M, Habuchi O, Yoshida K, Suzuki H, Ban K, Kimata K. The occurrence of three isoforms of heparan sulfate 6-O-sulfotransferase having different specificities for hexuronic acid adjacent to the targeted N- sulfoglucosamine. *J. Biol. Chem.*, **275**, 2859–2868 (2000).
18) Lu J, Auduong L, White ES, Yue X. Up-regulation of heparan sulfate 6-O-sulfation in idiopathic pulmonary fibrosis. *Am. J. Respir. Cell Mol. Biol.*, **50**, 106–114 (2014).
19) Condomitti G, De Wit J. Heparan sulfate proteoglycans as emerging players in synaptic specificity. *Front. Mol. Neurosci.*, **11** (2018).
20) Cole CL, Rushton G, Jayson GC, Avizienyte E. Ovarian cancer cell heparan sulfate 6-O-sulfotransferases regulate an angiogenic program induced by heparin-binding epidermal growth factor (EGF)-like growth factor/EGF receptor signaling. *J. Biol. Chem.*, **289**, 10488–10501 (2014).
21) Wang W, Ju X, Sun Z, Hou W, Yang L, Zhang R. Overexpression of heparan sulfate 6-O-sulfotransferase-2 enhances fibroblast growth factor-mediated chondrocyte growth and differentiation. *Int. J. Mol. Med.*, **36**, 825–832 (2015).
22) Nagai N, Habuchi H, Sugaya N, Nakamura M, Imamura T, Watanabe H, Kimata K. Involvement of heparan sulfate 6-O-sulfation in the regulation of energy metabolism and the alteration of thyroid hormone levels in male mice. *Glycobiology*, **23**, 980–992 (2013).
23) Duffield JS, Lupher M, Thannickal VJ, Wynn TA. Host responses in tissue repair and fibrosis. *Annu. Rev. Pathol. Mech. Dis*, **8**, 241–276 (2013).
24) Jackson AO, Zhang J, Jiang Z, Yin K. Endothelial-to-mesenchymal transition: A novel therapeutic target for cardiovascular diseases. *Trends Cardiovasc. Med.*, **27**, 383–393 (2017).